Korean J. Math. **33** (2025), No. 2, pp. 87–97
http://dx.doi.org/10.11568/kjm.2025.33.2.87

A NORMALIZED TIME-FRACTIONAL LOTKA–VOLTERRA MODEL

Junseok Kim

Abstract. In this study, we present a normalized time-fractional Lotka–Volterra model by using a normalized time-fractional derivative. To reflect memory property in biological systems, the time-fractional Lotka–Volterra model extends the traditional Lotka–Volterra system, which models predator-prey dynamics, by incorporating fractional calculus. The normalized fractional derivative possesses distinct advantages over existing fractional derivatives, notably the property that the sum of the weighting function equals 1. We provide a comprehensive description for a numerical solution algorithm of the proposed model and conduct computational simulations to illustrate the effects of varying the fractional order on predator-prey interactions. This study contributes to the ongoing development of fractional-order models in population dynamics and provides new insights into the behavior of predator-prey systems governed by fractional time evolution.

1. Introduction

The Lotka–Volterra model is a widely recognized framework for understanding predator-prey dynamics in ecological systems. It offers a simple yet effective way to examine how predator and prey populations change over time, which often shows cyclical patterns. This model provides valuable insights into population stability and the influence of various environmental factors. Its applications extend across fields such as microbiome research, conservation, and ecology [6], and recent studies have further explored its relevance in more complex ecosystems [17], including cancer cell competition [4] and microbial communities [5].

The time-fractional Lotka–Volterra model builds upon the classical version by incorporating fractional calculus, which allows for the representation of memory effects in biological systems [7]. This feature is especially important for systems where the current state depends not only on the present but also on past states, which offers a more accurate description of complex population dynamics [14, 18]. Fractional derivatives enhance the model's ability to capture long-range interactions and anomalous diffusion often observed in ecological systems. For instance, Owolabi [20] investigated equilibrium stability and Hopf bifurcation in a three-component time-fractional predator-prey model, while Jafari et al. [7] and Kumar et al. [13] applied Caputo–Fabrizio and Atangana–Baleanu operators and proposed numerical methods to analyze system behavior and stability. Ali et al. [1] investigated the existence, stability, and dynamics of a modified predator-prey model using the fractal–fractional order operator in the Caputo–Fabrizio sense and established stability conditions through nonlinear functional analysis and demonstrated that small immigrations

Received January 2, 2025. Accepted March 25, 2025. Publicated March 25, 2025.
2010 Mathematics Subject Classification: 34A08,65M06,92D25.
Key words and phrases: Normalized time-fractional Lotka–Volterra equation, predator-prey model, memory effect.

can stabilize predator-prey populations using numerical results. Jialin Chen et al. [2] studied a prey–predator model with a Holling-II function and created a stable nonlinear decision surface for binary classification, validated through experiments on synthetic and EEG signal data. For an overview of various predator–prey models that capture diverse behavioral dynamics in ecological systems, readers are referred to a recent review article [21].

Conventional time-fractional derivatives, however, are not normalized, as their weight functions do not sum to unity. To resolve this and provide a fair comparison in studying fractional order effects on evolutionary dynamics, this paper adopts a normalized time-fractional derivative for the Lotka–Volterra model.

The remainder of this article is organized as follows. In Section 2, we describe the proposed novel normalized Lotka–Volterra model. Section 3 presents a numerical solution algorithm. In Section 4, computational tests are performed. Section 5 provides a discussion. Section 6 concludes the paper with a summary.

2. Proposed normalized Lotka–Volterra model

The Lotka–Volterra equations, commonly referred to as the predator–prey model, are used to model the dynamics of biological systems involving two interacting species: one as the predator and the other as the prey. The population dynamics evolve over time based on these two equations:

$$\frac{du(t)}{dt} = \theta_1 u(t) - \theta_2 u(t)v(t), \tag{1}$$

$$\frac{dv(t)}{dt} = \theta_3 u(t)v(t) - \theta_4 v(t), \tag{2}$$

where $u(t)$ and $v(t)$ are the prey and predator at time t, respectively. The parameters $\theta_1,\ \theta_2,\ \theta_3$, and θ_4 are positive and represent the growth/decay rate of the population and the competition coefficients. The parameters θ_1 and θ_2 are the maximum per capita growth rate of the prey and the impact of predators on the prey's mortality rate, respectively. The parameters θ_3 and θ_4 correspond to the predator's per capita death rate and the influence of prey presence on the predator's growth rate [7]. In this study, we present a normalized time-fractional Lotka–Volterra model based on a normalized time-fractional derivative [8,15,16]:

$$\frac{d^\alpha u(t)}{dt^\alpha} = \theta_1 u(t) - \theta_2 u(t)v(t), \tag{3}$$

$$\frac{d^\alpha v(t)}{dt^\alpha} = \theta_3 u(t)v(t) - \theta_4 v(t), \tag{4}$$

where the normalized time-fractional is defined as follows:

$$\frac{d^\alpha u(t)}{dt^\alpha} = \frac{1-\alpha}{t^{1-\alpha}} \int_0^t \frac{du(s)}{ds} \frac{ds}{(t-s)^\alpha},\ 0 < \alpha < 1. \tag{5}$$

Here, the term $(1-\alpha)/t^{1-\alpha}$ preceding the integral in Eq. (5) is designed to normalize the derivative in the following sense. When $du(s)/ds = \beta$ is constant, then it follows that $d^\alpha u(t)/dt^\alpha = \beta$. In other words,

$$\frac{d^\alpha u(t)}{dt^\alpha} = \frac{1-\alpha}{t^{1-\alpha}} \int_0^t \beta \frac{ds}{(t-s)^\alpha} = \beta \frac{1-\alpha}{t^{1-\alpha}} \int_0^t \frac{ds}{(t-s)^\alpha} = \beta. \tag{6}$$

Furthermore, $d^\alpha v(t)/dt^\alpha$, is defined in a similar manner. Let $w_\alpha^t(s)$ be a weighting function:

$$w_\alpha^t(s) = \frac{1-\alpha}{t^{1-\alpha}(t-s)^\alpha}. \tag{7}$$

Then, we obtain

$$W_\alpha(t) = \int_0^t w_\alpha^t(s)ds = 1, \tag{8}$$

which depends on neither α nor t [10].

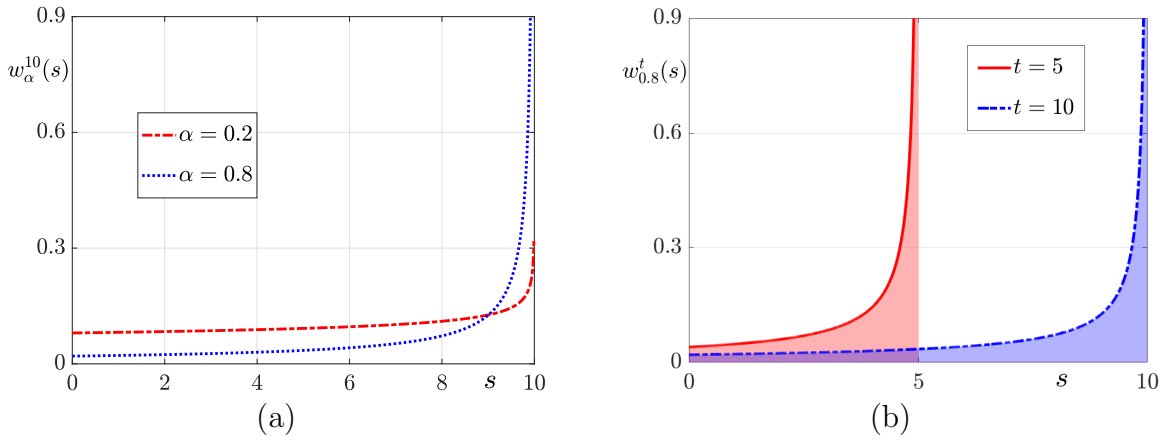

FIGURE 1. (a) $w_\alpha^{10}(s)$ for various α values with $t = 10$. (b) $w_{0.8}^t(s)$ for various t values with $\alpha = 0.8$.

Figure 1(a) shows the function $w_\alpha^{10}(s)$ plotted over interval $[0,\ 10)$ for two different values of α, specifically $\alpha = 0.2$ and $\alpha = 0.8$, while the parameter $t = 10$ is fixed. The red dashed line represents the plot for $\alpha = 0.2$, and the blue dotted line corresponds to $\alpha = 0.8$. Both curves show how $w_\alpha^{10}(s)$ evolves as s increases from 0 to 10. The curves exhibit a sharp rise as s approaches 10, particularly for larger values of α. Figure 1(b) displays the function $w_{0.8}^t(s)$ for two different values of t, specifically $t = 5$ and $t = 10$, while the parameter $\alpha = 0.8$ is held constant. The solid red line represents $w_{0.8}^5(s)$, and the blue dashed line represents $w_{0.8}^{10}(s)$. Both functions show an increasing trend as s approaches t. It is noted that the area under each curve (the filled region) is equal to one.

3. Computational method

Let $u_n = u(t_n)$ and $v_n = v(t_n)$ for $n = 1, \ldots,$ where $t_n = (n-1)\Delta t$. Equation (5), can be numerically solved as

$$\begin{aligned}
\frac{d^\alpha u(t_{n+1})}{dt^\alpha} &= \frac{1-\alpha}{t_{n+1}^{1-\alpha}} \sum_{p=1}^{n} \int_{t_p}^{t_{p+1}} \frac{du(s)}{ds} \frac{ds}{(t_{n+1}-s)^\alpha} \\
&\approx \sum_{p=1}^{n} \frac{1-\alpha}{t_{n+1}^{1-\alpha}} \int_{t_p}^{t_{p+1}} \frac{ds}{(t_{n+1}-s)^\alpha} \frac{u_{p+1}-u_p}{\Delta t} \\
&= \sum_{p=1}^{n} \frac{(n+1-p)^{1-\alpha} - (n-p)^{1-\alpha}}{n^{1-\alpha}} \frac{u_{p+1}-u_p}{\Delta t}.
\end{aligned} \tag{9}$$

Hence, we obtain for Eqs. (3) and (4) using Eq. (9):

$$\sum_{p=1}^{n} w_p^n \frac{u_{p+1}-u_p}{\Delta t} = \theta_1 u_{n+1} - \theta_2 u_{n+1} v_n, \tag{10}$$

$$\sum_{p=1}^{n} w_p^n \frac{v_{p+1}-v_p}{\Delta t} = \theta_3 u_n v_{n+1} - \theta_4 v_{n+1}, \tag{11}$$

where $w_p^n = [(n+1-p)^{1-\alpha} - (n-p)^{1-\alpha}]/n^{1-\alpha}$, which satisfies

$$\sum_{p=1}^{n} w_p^n = 1. \tag{12}$$

We rewrite the discrete system of Eqs. (10) and (11) as follows:

$$u_{n+1} = u_n + \frac{\Delta t}{w_n^n}\left(\theta_1 u_{n+1} - \theta_2 u_{n+1} v_n - \sum_{p=1}^{n-1} w_p^n \frac{u_{p+1}-u_p}{\Delta t}\right), \tag{13}$$

$$v_{n+1} = v_n + \frac{\Delta t}{w_n^n}\left(\theta_3 u_n v_{n+1} - \theta_4 v_{n+1} - \sum_{p=1}^{n-1} w_p^n \frac{v_{p+1}-v_p}{\Delta t}\right). \tag{14}$$

We reformulate the discrete system given by Eqs. (13) and (14) in the following manner:

$$u_{n+1} = \left(u_n - \frac{\Delta t}{w_n^n}\sum_{p=1}^{n-1} w_p^n \frac{u_{p+1}-u_p}{\Delta t}\right) \Big/ \left(1 - \frac{\Delta t(\theta_1 - \theta_2 v_n)}{w_n^n}\right), \tag{15}$$

$$v_{n+1} = \left(v_n - \frac{\Delta t}{w_n^n}\sum_{p=1}^{n-1} w_p^n \frac{v_{p+1}-v_p}{\Delta t}\right) \Big/ \left(1 - \frac{\Delta t(\theta_3 u_n - \theta_4)}{w_n^n}\right). \tag{16}$$

4. Computational experiments

We consider a set of test problems similar to those discussed in detail in [9], where a comprehensive analysis of comparable cases was conducted. By using these test cases, we want to assess the effectiveness and applicability of the proposed model in a manner consistent with the prior study. This allows for a comparison of results and provides a clearer understanding of the improvements introduced in the current study.

Figure 2 shows the computational results of prey-predator dynamics for different values of the parameter α, obtained by solving the discrete Eqs. (15) and (16) with initial conditions $u(0) = 1.3$ and $v(0) = 0.6$. Figures 2(a), (b), (c), and (d) correspond to values of α equal to 0.3, 0.8, 0.95, and 1, respectively. In these plots, $u(t)$ is the prey population (solid blue line), while $v(t)$ is the predator population (dashed red line), both as functions of time t. The dynamics vary significantly with different α values. For smaller α values (e.g., in Fig. 2(a)), the system tends toward a steady state, where the predator and prey populations stabilize after a few oscillations. In Fig. 2(b) and (c), as α increases to 0.8 and 0.95, the oscillations persist longer, which indicate more extended interactions between predator and prey. It is noted that the amplitude of the oscillations decreases in both cases. Figure 2(d), where α equals 1, shows increasingly pronounced, sustained, and periodic oscillations, which suggests a less stable dynamic system. Here, the values $\theta_1 = \theta_2 = \theta_3 = \theta_4 = 1$ and $\Delta t = 0.001$ are used. The increasing amplitude and persistence of oscillations with higher α values highlight the effect of α on system stability and predator-prey interaction. The computational results illustrate that as α increases, the system shifts from a stable

equilibrium to a more oscillatory and potentially unstable dynamic, with prey and predator populations fluctuating over time rather than converging to a constant value.

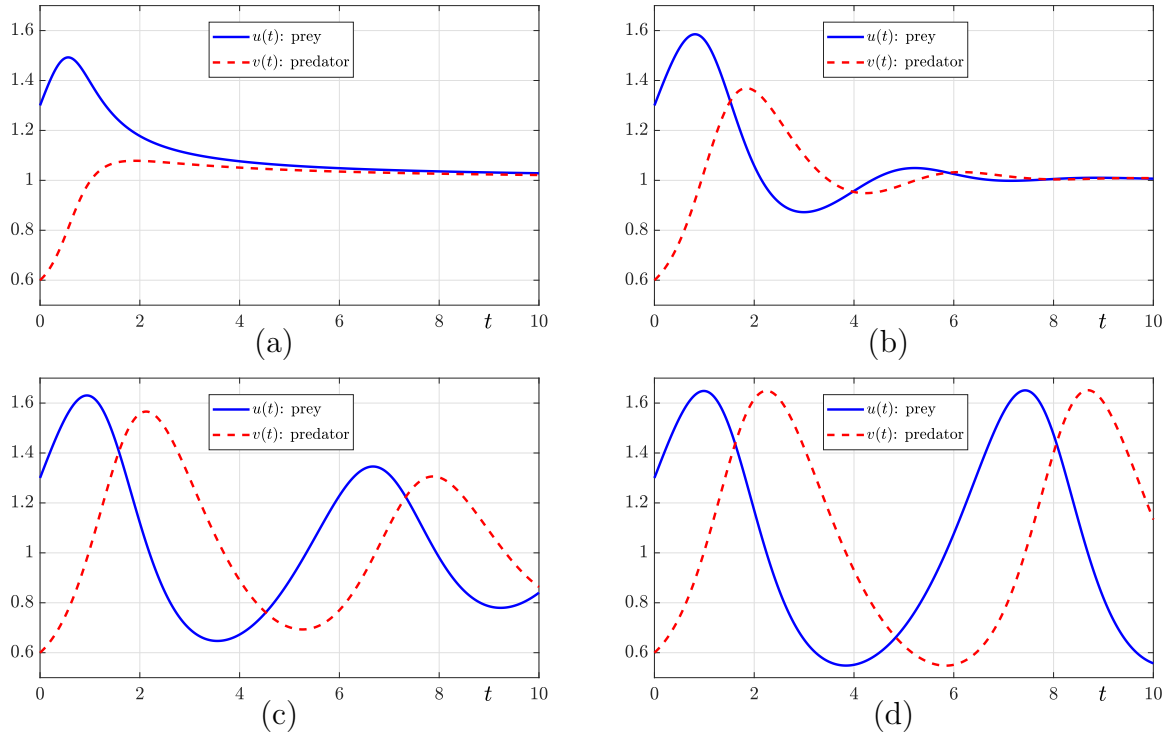

FIGURE 2. (a), (b), (c), and (d) are the numerical results for $\alpha = 0.3,\ 0.8,\ 0.95$, and 1, respectively. Here, $\theta_1 = \theta_2 = \theta_3 = \theta_4 = 1$ are used.

Figure 3 illustrates the computational results for predator-prey dynamics using the normalized time-fractional Lotka–Volterra model for various values of the fractional parameter $\alpha = 0.3,\ 0.8,\ 0.95$, and 1.0, with three different initial conditions: $u(0) = 1.3$, $v(0) = 0.6$; $u(0) = 1.7$, $v(0) = 1.3$; and $u(0) = 0.5$, $v(0) = 1.5$. Figures 3(a), (b), (c), and (d) represent the dynamics for each of these α values. For $\alpha = 0.3$, the trajectories from the three initial conditions display a spiral pattern, converging to a stable equilibrium point. The system quickly stabilizes, with less pronounced oscillations, as shown in Fig. 3(a). As α increases to 0.8, the system exhibits more sustained oscillations compared to $\alpha = 0.3$, as illustrated in Fig. 3(b). The trajectories spiral inward more gradually, which indicates slower convergence to the equilibrium point. The system maintains a more complex predator-prey interaction before stabilizing. At $\alpha = 0.95$, the oscillations become more pronounced, with the trajectories completing additional loops before converging. The slower inward spiral, as shown in Fig. 3(c), suggests a stronger influence of memory effects and delays stabilization and extending the oscillatory phase. For $\alpha = 1.0$, the trajectories form closed orbits rather than converging to a fixed point. This is the classical Lotka–Volterra behavior, where predator-prey populations undergo perpetual cycles without damping. The dynamics maintain stable, periodic oscillations and this behavior reflects a persistent predator-prey interaction that does not settle into a steady state, as displayed in Fig. 3(d). As α increases, the system's oscillatory behavior becomes more pronounced, with slower convergence toward equilibrium. The initial conditions affect the trajectories when α is less than 1, with all trajectories converging to the equilibrium point. However, when $\alpha = 1$, the system forms closed loops that pass through the initial points and it results in persistent cycles. As α decreases, the fractional effects become more pronounced and it leads to slower convergence, which highlights the increased influence of memory effects in the system. This

analysis highlights the impact of the fractional parameter α on the system's memory and the dynamics of predator-prey interactions.

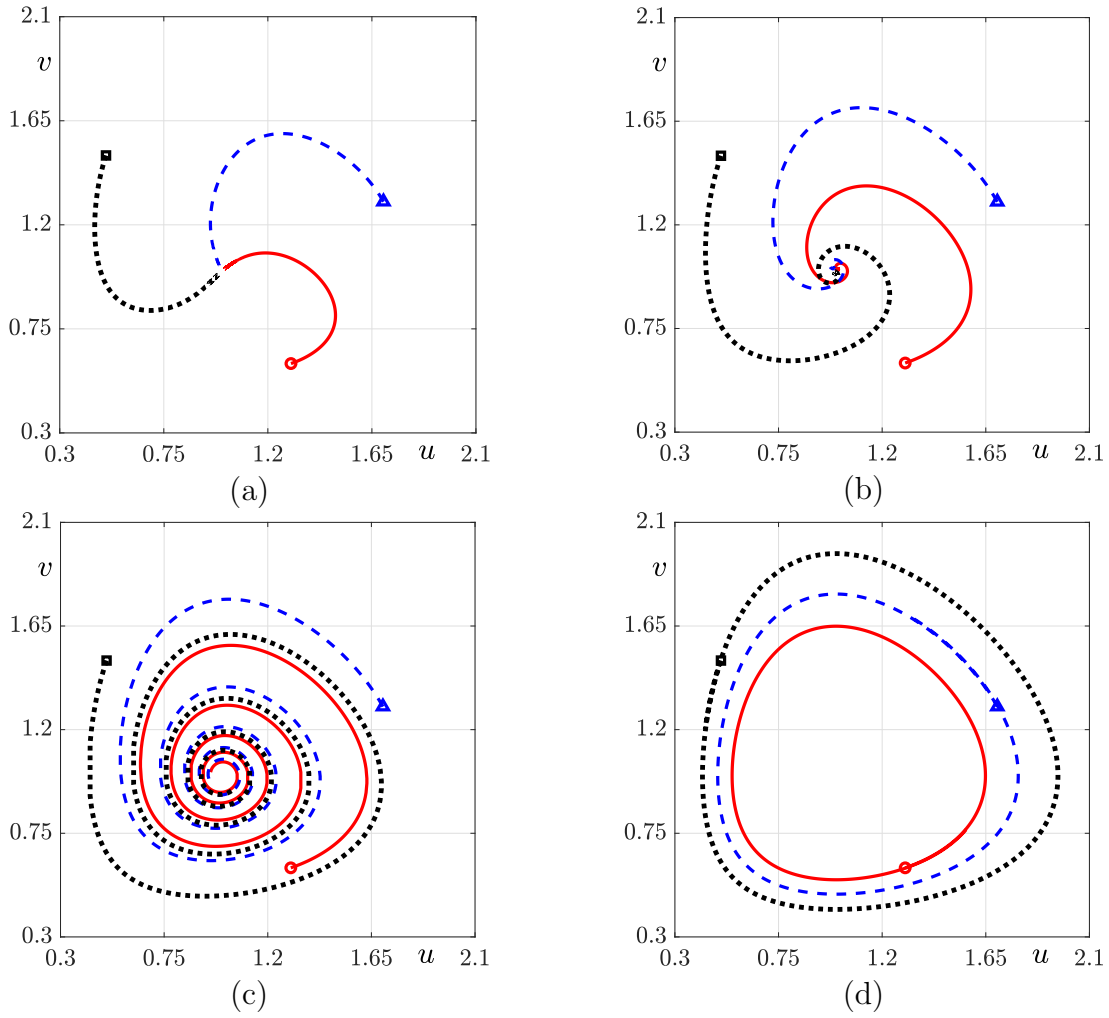

FIGURE 3. (a), (b), (c), and (d) are the numerical results for different values of $\alpha = 0.3,\ 0.8,\ 0.95$, and 1, respectively, with three initial conditions, $(u(0), v(0)) = (1.3, 0.6),\ (1.7, 1.3)$, and $(0.5, 1.5)$. Here, $\theta_1 = \theta_2 = \theta_3 = \theta_4 = 1$ are used. The temporal evolution is observed up to time $t = 25$.

Figures 4(a), (b), (c), and (d) show numerical results for different values of the parameter α and represent the dynamics of a prey-predator model. The variables $u(t)$ and $v(t)$ are prey and predator populations, respectively, as indicated by the legend in each plot. The curves show the evolution of these populations over time t, from 0 to 20. Figures 4(a) to (d) correspond to different values of α: (a) $\alpha = 0.3$, (b) $\alpha = 0.8$, (c) $\alpha = 0.95$, and (d) $\alpha = 1$. The solid blue line is the prey population $u(t)$ over time, while the dashed red line is the predator population $v(t)$ over time. In Fig. 4(a), the prey and predator populations quickly stabilize at a lower steady-state value. In Fig. 4(b), the prey and predator populations exhibit some oscillatory behavior before approaching steady states. In Fig. 4(c), more persistent oscillations are observed and gradually approaching a steady state. In Fig. 4 (d), the oscillations become more pronounced and indicates cyclical dynamics between the prey and predator populations. Low α values, as shown in Fig. 4(a), result in damped behavior, with both prey and predator populations stabilizing at steady-state values over time. In contrast, higher α values, such as in Figs. 4(c) and (d), lead to more pronounced

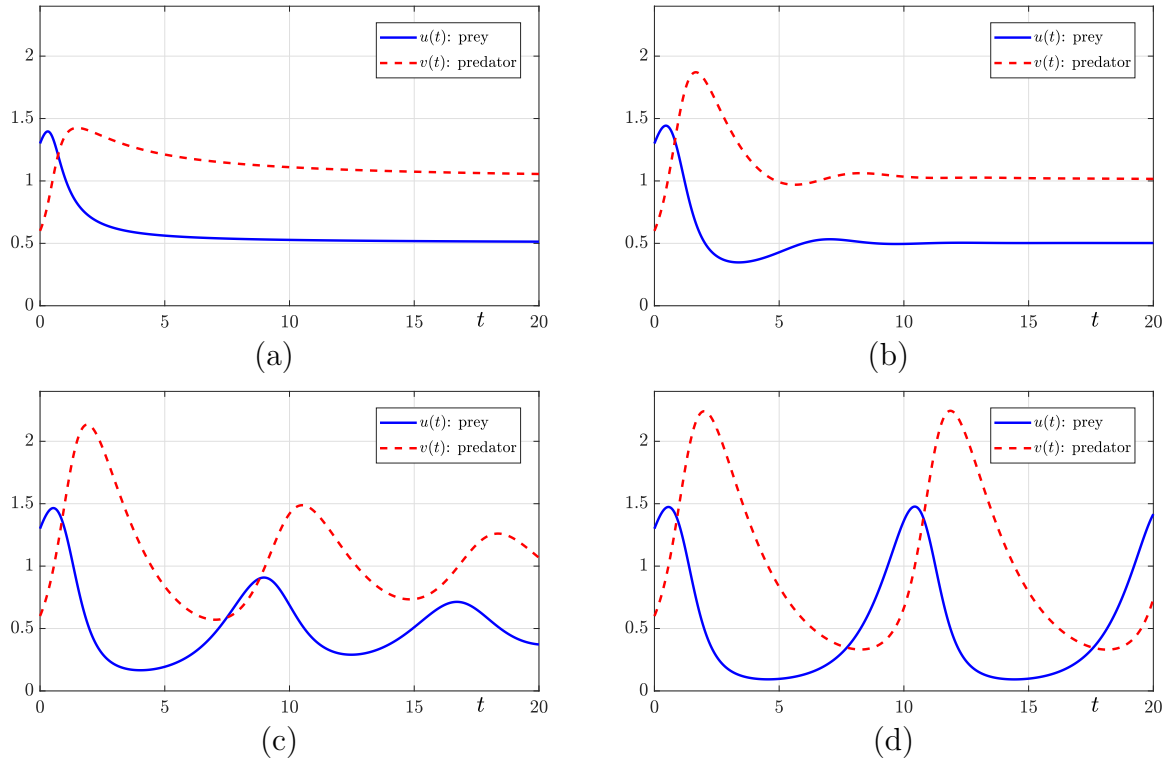

FIGURE 4. (a), (b), (c), and (d) are the numerical results for $\alpha = 0.3$, 0.8, 0.95, and 1, respectively. Here, $\theta_1 = \theta_2 = \theta_3 = 1$ and $\theta_4 = 0.5$ are used.

oscillatory dynamics, where both populations experience repeated cycles of growth and decline. Specifically, Fig. 4(d) highlights stronger predator-prey interactions and shows periodic fluctuations in population sizes. The parameter α influences the intensity and frequency of these oscillations, with larger α producing more prominent periodic behavior. These computational results demonstrate the time evolution of a prey-predator model under varying α values. As α increases, the system transitions from a stable state with minimal oscillations (Fig. 4(a)) to more dynamic, cyclical population interactions (Figs. 4(c) and (d)), following typical predator-prey dynamics.

Figure 5 shows the phase plane dynamics for different values of the parameter α. The system's temporal evolution is observed up to time $t = 25$, with three different initial conditions: $(u(0), v(0)) = (1.3, 0.6), (1.7, 1.3)$, and $(0.5, 1.5)$, as marked by the different symbols (circle, square, and triangle) on each plot. In Fig. 5(a), with $\alpha = 0.3$, the trajectories approach a steady state where the populations stabilize. The inward spiral orbits indicate that both the prey (u) and predator (v) populations gradually reach equilibrium without continued cycles. In Fig. 5(b), with ($\alpha = 0.8$), the oscillations persist longer than in Fig. 5(a), with trajectories spiraling toward the steady-state solution more slowly. The system shows oscillatory behavior but eventually approaches equilibrium, though more gradually than in the previous case. In Fig. 5(c), with ($\alpha = 0.95$), the system displays more persistent oscillations, where the trajectories take significantly more time to settle down to a steady state. The oscillations are more prominent than in Figs. 5 (a) and (b), which indicates that increasing α introduces more pronounced dynamic interactions between the populations before reaching equilibrium. In Fig. 5(d), with ($\alpha = 1$), this case represents periodic behavior, where the populations of prey and predator exhibit closed orbits in the phase space, which indicates sustained cycles with no decay in amplitude. The populations repeatedly rise and fall in a cyclic manner, which suggests a balanced predator-prey

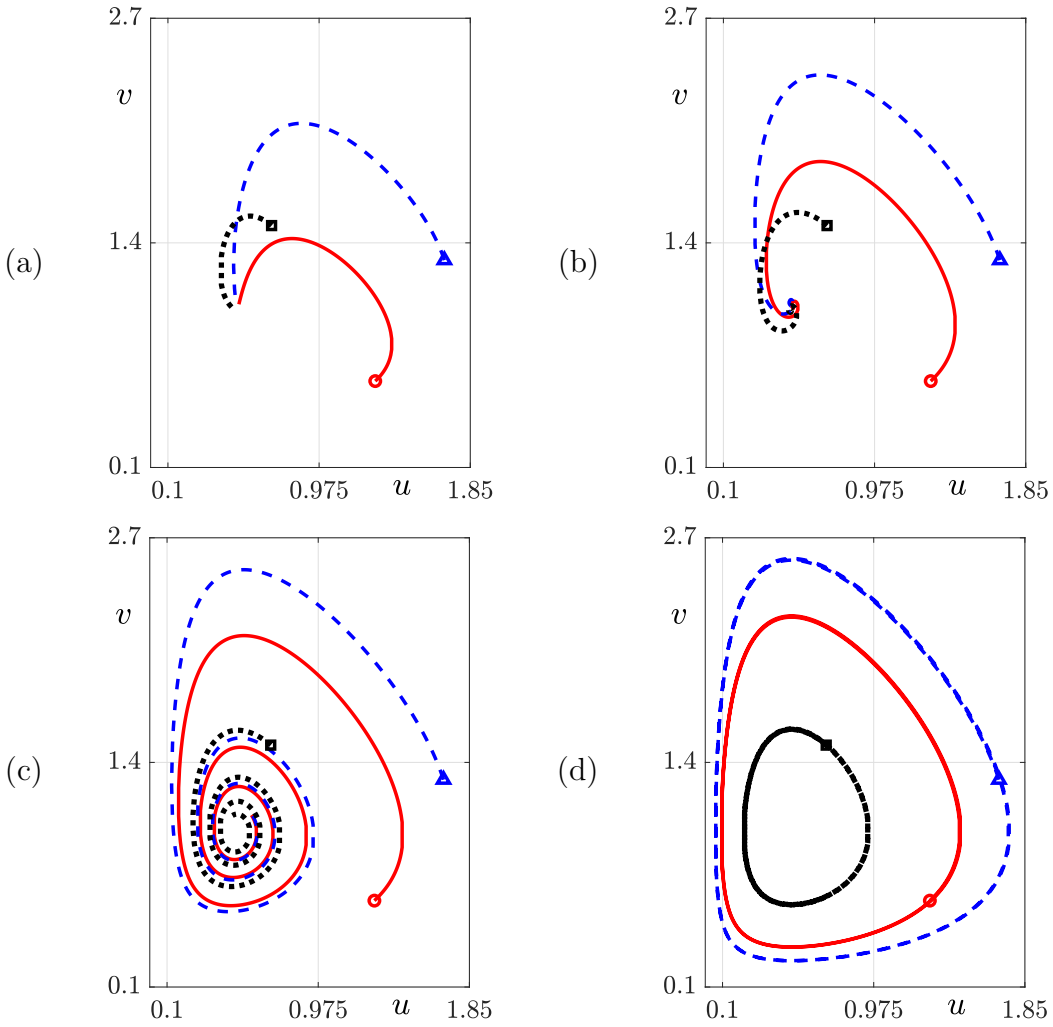

FIGURE 5. (a), (b), (c), and (d) are the numerical results for $\alpha = 0.3,\ 0.8,\ 0.95$, and 1, respectively, with three initial conditions, $(u(0), v(0)) = (1.3, 0.6),\ (1.7, 1.3)$, and $(0.5, 1.5)$. Here, $\theta_1 = \theta_2 = \theta_3 = 1$ and $\theta_4 = 0.5$ are used. The temporal evolution is observed up to time $t = 25$.

relationship without approaching a steady state. As α increases from 0.3 to 1, the system transitions from damped oscillations and steady states (Fig. 5(a)) to more persistent oscillations (Fig. 5(c)), and finally to periodic, sustained cycles (Fig. 5(d)). The parameter α controls the strength and persistence of the oscillations, with larger α values leading to a shift from damped dynamics to periodic behavior.

5. Discussion

The numerical method used in this study provides an efficient and stable framework for simulating the dynamics of the normalized time-fractional Lotka–Volterra system. By discretizing the normalized fractional derivative using a convolution-type quadrature with the normalized weights, the method ensures that the memory effects intrinsic to fractional dynamics are accurately captured. A notable feature of the proposed algorithm is that the discretized weights sum to unity, which preserves the normalization property. The update formulation introduced in equations Eqs. (15) and (16) avoids solving fully implicit systems, which reduces computational complexity. The scheme exhibits robustness under

various fractional orders $\alpha \in (0, 1]$, and numerical experiments confirm that it can handle both stiff and oscillatory regimes inherent to predator–prey systems. For small values of α, the method successfully simulates damped dynamics, while for $\alpha \approx 1$, it reproduces periodic behavior consistent with classical Lotka–Volterra cycles. The numerical results indicate that the algorithm maintains stability and accuracy across a wide range of initial conditions and parameter choices. Moreover, the computational experiments demonstrate that the algorithm captures the transition between asymptotically stable and persistent oscillatory regimes as the fractional parameter increases. This confirms the method's capability to resolve long-term behavior and delayed stabilization phenomena, which are typical in memory-governed ecological models. Overall, the numerical scheme not only supports the theoretical formulation of the normalized time-fractional model but also offers a reliable tool for further studies involving generalized memory effects in nonlinear dynamical systems.

6. Conclusions

In this paper, we presented a normalized time-fractional Lotka–Volterra model to investigate the dynamics of predator-prey interactions by incorporating fractional calculus. Our model, which uses a normalized time-fractional derivative, accounts for the memory effects observed in biological systems. Through comprehensive computational experiments, we demonstrated that the fractional parameter α significantly influences the system's behavior, with lower values leading to damped oscillations and stable steady states, while higher values result in more persistent and periodic oscillations. The results highlight the critical role of α in controlling the intensity and frequency of oscillations in predator-prey dynamics, which offer a more flexible and realistic representation of complex population interactions. The findings of this paper will be useful to research on fractional-order models and provide important insights into the application of fractional calculus in ecological systems. In future work, we will extend the current study to a higher-dimensional time-fractional Lotka–Volterra model [19], to space-dependent population dynamics [3], to population dynamics [12], and to the analysis of pattern formation in the Lengyel–Epstein system [11].

Appendix

The following MATLAB code implements the proposed normalized time-fractional Lotka–Volterra model. This will be useful for those who wish to implement the code for simulating and analyzing predator-prey dynamics within a fractional-order framework. This code illustrates the numerical solution of the normalized time-fractional Lotka–Volterra model, which expands the classical model by introducing normalized fractional derivatives to capture memory effects in the interactions between predator and prey populations.

Listing 1. MATLAB program

```
clear; clf;
T=10; dt=0.001; Nt=round(T/dt);
u=zeros(Nt,1); % prey
v=u;           % predator
t1=1; t2=1; t3=1; t4=1;
u(1)=1.3; v(1)=0.8;
flag=2;    % flag=1 is alpha=1 and flag2 is 0<alpha<1
beta = 0.95;
for n = 1:Nt
    deno = n^(1-beta);
```

```
    for p = 1:n
        w(p) = ((n+1-p)^(1-beta)-(n-p)^(1-beta))/deno;
    end
    F1=0; F2=0;
    if n > 1
        for p = 1:n-1
            F1 = F1+w(p)*(u(p+1)-u(p))/dt;
            F2 = F2+w(p)*(v(p+1)-v(p))/dt;
        end
    end
    if flag==1
    u(n+1)=u(n)+dt*u(n)*(t1-t2*v(n));
    v(n+1)=v(n)+dt*v(n)*(t3*u(n)-t4);
    else
     coefu=1-dt*(t1-t2*v(n))/w(n);
    u(n+1)=(u(n)-(dt/w(n))*F1)/coefu;
     coefv=1-dt*(t3*u(n)-t4)/w(n);
    v(n+1)=(v(n)-(dt/w(n))*F2)/coefv;
    end
end
t=linspace(0,Nt*dt,Nt+1);
plot(t,u,'b-','linewidth',2); hold on
plot(t,v,'r--','linewidth',2); grid on
xlabel('t');  legend('u(t)','v(t)')
axis([0 10 0.5 1.7]);
```

References

[1] Z. Ali, F. Rabiei, K. Hosseini, *A fractal–fractional-order modified predator-prey mathematical model with immigrations*, Math. Comput. Simul. **207** (2023), 466–481.
https://doi.org/10.1016/j.matcom.2023.01.006

[2] J. Chen, X. Chen, J. Wang, *A novel binary data classification algorithm based on the modified reaction–diffusion predator-prey system with Holling-II function*, Chaos **34**(10) (2024), 103111.
https://doi.org/10.1063/5.0219960

[3] M. Chen, S. Ham, J. Kim, *Taxis-driven complex patterns of a plankton model*, Chaos **34**(6) (2024), 063101.
https://doi.org/10.1063/5.0195576

[4] H. Cho, A.L. Lewis, K.M. Storey, H.M. Byrne, *Designing experimental conditions to use the Lotka–Volterra model to infer tumor cell line interaction types*, J. Theor. Biol. **559** (2023), 111377.
https://doi.org/10.1016/j.jtbi.2022.111377

[5] J.D. Davis, D.V. Olivença, S.P. Brown, E.O. Voit, *Methods of quantifying interactions among populations using Lotka–Volterra models*, Front. Syst. Biol. **2** (2022), 1021897.
https://doi.org/10.3389/fsysb.2022.1021897

[6] Z. Eskandari, Z. Avazzadeh, G. Khoshsiar, B. Li, *Dynamics and bifurcations of a discrete-time Lotka–Volterra model using nonstandard finite difference discretization method*, Math. Methods Appl. Sci. **48** (2022), 7197–7212.
https://doi.org/10.1002/mma.8859

[7] H. Jafari, R.M. Ganji, N.S. Nkomo, Y.P. Lv, *A numerical study of fractional order population dynamics model*, Results Phys. **27** (2021), 104456.
https://doi.org/10.1016/j.rinp.2021.104456

[8] M. Jornet, J.J. Nieto, *Power-series solution of the L-fractional logistic equation*, Appl. Math. Lett. **154** (2024), 109085.
https://doi.org/10.1016/j.aml.2024.109085

[9] A.R. Kanth, S. Devi, *A practical numerical approach to solve a fractional Lotka–Volterra population model with non-singular and singular kernels*, Chaos Solitons Fractals **145** (2021), 110792.
https://doi.org/10.1016/j.chaos.2021.110792

[10] J. Kim, *Influence of fractional order on the behavior of a normalized time-fractional SIR model*, Mathematics **12** (2024), 3081.
https://doi.org/10.3390/math12193081

[11] H. Kim, Jyoti, S. Kwak, S. Ham, J. Kim, *In silico investigation of the formation of multiple intense zebra stripes using extending domain*, Math. Comput. Simul. **225** (2024), 648–658.
https://doi.org/10.1016/j.matcom.2024.06.010

[12] M. Kim, Y. Kim, C. Oh, *Intervention strategies for the dynamics of population with overeating behavior*, J. KSIAM **27**(2) (2023), 123–134.
https://doi.org/10.12941/jksiam.2023.27.123

[13] A. Kumar, S. Kumar, S. Momani, S. Hadid, *A chaos study of fractal–fractional predator–prey model of mathematical ecology*, Math. Comput. Simul. **225** (2024), 857–888.
https://doi.org/10.1016/j.matcom.2023.09.010

[14] H. Kumar, *Numerical solution of Abel's general fuzzy linear integral equations by fractional calculus method*, Korean J. Math. **29**(3) (2021), 527–545.
https://doi.org/10.11568/kjm.2021.29.3.527

[15] K.A. Lazopoulos, A.K. Lazopoulos, *Fractional vector calculus and fractional continuum mechanics*, Progr. Fract. Differ. Appl. **2** (2016), 67–86.
https://doi.org/10.18576/pfda/020202

[16] C. Lee, Y. Nam, M. Bang, S. Ham, J. Kim, *Numerical investigation of the dynamics for a normalized time-fractional diffusion equation*, AIMS Math. **9** (2024), 26671–26687.
https://doi.org/10.3934/math.20241297

[17] Y. Li, Z. Lv, Q. Xia, *On the adaption of biological transport networks affected by complex domains*, Phys. Fluids **36**(10) (2024), 103106.
https://doi.org/10.1063/5.0231079

[18] A. Mohanapriya, V. Sivakumar, P. Prakash, *A generalized approach of fractional Fourier transform to stability of fractional differential equation*, Korean J. Math. **29**(4) (2021), 749–763.
https://doi.org/10.11568/kjm.2021.29.4.749

[19] M.K. Naik, C. Baishya, P. Veeresha, *A chaos control strategy for the fractional 3D Lotka–Volterra like attractor*, Math. Comput. Simul. **211** (2023), 1–22.
https://doi.org/10.1016/j.matcom.2023.04.001

[20] K.M. Owolabi, *Computational study of noninteger order system of predation*, Chaos **29**(1) (2019), 013120.
https://doi.org/10.1063/1.5079616

[21] K. Singh, T. Singh, L.N. Mishra, R. Dubey, L. Rathour, *A brief review of predator–prey models for an ecological system with a different type of behaviors*, Korean J. Math. **32**(3) (2024), 381–406.
https://doi.org/10.11568/kjm.2024.32.3.381

Junseok Kim
Department of Mathematics, Korea University, Seoul 02841, Republic of Korea
E-mail: cfdkim@korea.ac.kr